







Improving Properties of Wood-plastic Composites with High-density Reinforcements under Water Immersion

Sriwan Khamtree ^a, Santi Khamtree ^b, Chainarong Srivabut ^c,
Uraiwan Sookyung ^c, Tanetpon Chookham,^c Prutipong Pantamanatsopa ^c,
and Chatree Homkhiew ^{c,*}

Effects of high-density agricultural by-product fillers, coconut shell flour (CSF), and palm kernel shell flour (PKSF) were investigated relative to the physical and mechanical properties after water immersion of wood-plastic composites (WPCs), compared to conventional rubberwood flour (RWF). The WPCs were fabricated with filler contents of 30, 40, and 50 wt% and subjected to long-term water immersion for 8 weeks. Morphological analyses revealed that CSF and PKSF particles exhibited denser and more angular structures than RWF, thereby enhancing filler-matrix interfacial compatibility. Mechanical testing showed that modulus of rupture decreased with increasing filler content while modulus of elasticity increased, and RWF composites yielded the highest initial strength. Under prolonged water exposure, CSF-filled composites exhibited the lowest degradation in flexural strength, screw withdrawal resistance, hardness, and surface quality, which can be attributed to CSF's high lignin content and structural compactness. Further, RWF-filled composites showed the most considerable deterioration. Water absorption and thickness swelling were lowest in CSF composites, confirming superior dimensional stability. These findings underscore the potential of CSF and PKSF as sustainable reinforcements to improve WPC durability in moist environments, supporting circular material utilization from agricultural residues.

DOI: 10.15376/biores.21.1.1030-1049

Keywords: Wood-plastic composites; Water absorption; Rubberwood; Coconut shell; Palm kernel shell

Contact information: a: Faculty of Industrial Technology, Songkhla Rajabhat University, Songkhla 90000, Thailand; b: Faculty of Industrial Technology, Nakhon Si Thammarat Rajabhat University, Nakhon Si Thammarat, 80280 Thailand; c: Materials Processing Technology Research Unit, Faculty of Engineering, Rajamangala University of Technology Srivijaya, Songkhla 90000, Thailand;

* Corresponding author: chatree.h@rmutsv.ac.th

INTRODUCTION

Wood-plastic composites (WPCs) are increasingly utilized in construction, automotive, and furniture applications due to their favorable mechanical properties, ease of processing, and recyclability (Ayrilmis *et al.* 2012; Bal 2022). Through combining thermoplastic matrices with lignocellulosic fillers, WPCs achieve greater stiffness and dimensional stability compared with neat polymers, while maintaining flexibility in design and manufacturing (Homkhiew *et al.* 2024; Srivabut *et al.* 2024). Nevertheless, their long-term performance in humid or submerged environments remains restricted by moisture susceptibility, which deteriorates mechanical properties, dimensional stability, and surface quality (Mysiukiewicz and Sterzyński 2017; Ratanawilai and Srivabut 2022). Moisture penetration accelerates interfacial debonding between hydrophilic fillers and hydrophobic

polymer matrices, leading to progressive reductions in strength, modulus, hardness, and surface quality (Islam and Hasan 2025; Khamtree *et al.* 2023).

Numerous approaches have been explored to improve the moisture resistance of WPCs, including coupling agents, matrix and fiber modifications, nanofillers, and alternative natural fibers (Olonisakin *et al.* 2022; Ejeta 2023; Ayrlmis *et al.* 2025). Silane treatments can enhance filler-matrix adhesion and reduce water uptake (Daud *et al.* 2016), while inorganic nanoparticles, such as magnesium oxide and titanium dioxide can contribute further to water barrier properties (Guo *et al.* 2021; Ayrlmis *et al.* 2025). Chen *et al.* (2025) revealed that WPC-lumber co-extrusion composites offer the waterproofing and anti-degradative characteristics to WPCs. Alternative lignocellulosic fillers, including walnut shell flour (Bal 2023) and luffa fiber (Bera *et al.* 2019), have also been examined for their distinctive morphologies and relatively hydrophobic tendencies. However, high-density agricultural by-products, such as coconut shell (CS) and palm kernel shell (PKS), have remained underexplored, despite their abundance and promising physical characteristics for mitigating moisture-induced degradation. Both CS and PKS are characterized by high lignin contents (46.0% and 50.5%, respectively) and densities of 1,310 kg/m³ and 1,254 kg/m³, respectively (Dagwa and Ibhádode 2008; Sekhon *et al.* 2021; Anuchi *et al.* 2022). These attributes impart hydrophobicity and structural compactness, which may reduce porosity, restrict water diffusion, and enhance dimensional stability during immersion. Although CS and PKS have been studied in natural rubber and thermoset matrices (Daud *et al.* 2016; Anuchi *et al.* 2022), their application as high-density reinforcements in WPCs remains largely unexamined. Furthermore, systematic evaluations of filler density and morphology on interfacial bonding and mechanical retention under prolonged water exposure are still limited (Gamstedt *et al.* 2011; Islam and Hasan 2025). Addressing this knowledge gap is essential, as utilizing such agricultural by-products has the potential to simultaneously improve the moisture durability of WPCs and advance waste valorization within circular material systems (Homkhiew *et al.* 2024). Therefore, the novelty of this study lies in the introduction of CSF and PKSF as high-density reinforcements for WPCs, focusing on their influence on water resistance and mechanical retention under long-term immersion. Unlike previous studies that primarily employed low- to medium-density lignocellulosic fillers. This research systematically examines the effect of filler density and morphology on interfacial integrity and dimensional stability. The findings are expected to provide new insights into the role of high-lignin, high-density agricultural residues in enhancing the moisture durability and service performance of WPCs, while contributing to sustainable utilization of agro-industrial waste.

The present work aimed to investigate the effect of high-density agricultural by-product fillers, CS flour, and PKS flour, on physical and mechanical properties after water immersion of high-density polyethylene-based WPCs, compared to conventional rubberwood flour (RWF). The ultimate goal of the work was to improve physical and mechanical properties of WPCs under prolonged water exposure. The analysis includes water absorption, thickness swelling, and degradation in modulus of rupture (MOR), modulus of elasticity (MOE), screw withdrawal strength (SWS), hardness, and surface roughness during long-term water immersion. By linking filler properties with durability outcomes, this research addresses a critical deficiency in WPC development and contributes to the design of sustainable composites with enhanced resistance to moisture-induced degradation, thereby extending their suitability for outdoor and structural applications.

EXPERIMENTAL

Materials

High density polyethylene (trade name HD6600B), exhibiting a melt flow rate of 0.40 g/10 min at 190 °C under load of 2.16 kg and density of 0.957 g/cm³, were procured from PTT Global Chemical Public Co., Ltd. (Bangkok, Thailand) and utilized as the plastic matrix. Three types of reinforcement materials were examined: rubberwood flour, coconut shell, and palm kernel shell. Rubberwood flour was sourced from polishing residues generated by a Plan Creations Co., Ltd. (Trang, Thailand). Coconut shell was supported from a local coconut processing plant (Songkhla, Thailand). Palm kernel shell was supplied by a Kaset Lumnam Co., Ltd. (Nakhon Si Thammarat, Thailand). Before manufacturing, both coconut shell and palm kernel shell were processed into fine particles using a hammer mill (Model YLFJ-20B, BONNY), as illustrated in Fig. 1. Subsequently, the milled particles and rubberwood flour were sieved through a standard size 80-mesh sieve (passing particles smaller than 177 μ m), and then oven-dried at 100 °C for 24 h. The chemical composition and density of each reinforcement material are presented in Table 1.



Fig. 1. Coconut shell and palm kernel shell flours

Table 1. Chemical Composition and Density of Each Reinforcement Material

Reinforcement Material	Chemical Composition (%)				Density (kg/m ³)
	Cellulose	Hemicellulose	Lignin	Ash	
Rubberwood	39.0 ^a	29.0 ^a	28.0 ^a	4.0 ^a	480-650 ^d
Coconut shell	25.2 ^b	27.7 ^b	46.0 ^b	0.1 ^b	1,310 ^e
Palm kernel shell	28.8 ^c	22.7 ^c	50.5 ^c	1.0 ^c	1,254 ^f

Note: a: Petchpradab *et al.* 2009; b: Anuchi *et al.* 2022; c: Daud *et al.* 2016; d: Lim *et al.* 2003; e: Sekhon *et al.* 2021; f: Dagwa *et al.* 2008

Composites Processing

The production of the WPCs was completed in two sequential stages. In the first stage, high density polyethylene (HDPE) and reinforcement materials, such as rubberwood flour (RWF), coconut shell flour (CSF), and palm kernel shell flour (PKSF), were compounded using a twin-screw extruder (Model CTE-D25L40, Chareon Tut Co., Ltd., Samut Prakan, Thailand), as shown the formulations in Table 2. The temperature settings for the seven heating zones of the twin-screw extruder were maintained within the range of 175 to 190 °C, while the screw rotation speed during the blending process was regulated at 60 rpm. The extruded strands were subsequently pelletized using a cutting machine to produce WPC pellets. Following compounding, the pellets were oven-dried at 110 °C for 8 h to remove residual moisture. In the second stage, the dried pellets were molded into WPC panels using a compression molding machine. The panels were fabricated with dimensions of 200 mm in width, 250 mm in length, and 4.8 mm in thickness. The molding process was

conducted at a constant temperature of 190 °C under a maximum pressure of 10.34 MPa (1500 psi) for a total duration of 15 min, comprising a 5-min preheating stage and a 10-min compression stage. Finally, the molded WPC panels were cut into test specimens, as displayed in Fig. 2, with standardized dimensions according to the applicable American Society for Testing and Materials (ASTM) procedures for mechanical and physical property evaluation.



Fig. 2. Test specimens of WPCs for testing (a) flexure, (b) water absorption, (c) screw withdrawal, (d) surface roughness, and (e) hardness

Water Absorption Testing

Long-term water absorption (WA) and thickness swelling (TS) of the WPC specimens were evaluated in accordance with ASTM D 570-98 (1998). For each formulation, five replicate specimens were prepared by cutting from WPC panels into rectangle samples measuring 10 mm × 20 mm × 4.8 mm. Prior to testing, the specimens were oven-dried at 50 °C for 24 h to minimize residual moisture. The initial weight and thickness of each sample were measured with a precision of 0.0001 g and 0.001 mm, respectively. Subsequently, the specimens were fully immersed in distilled water at room temperature for a duration of 8 weeks. Every 2 weeks, the samples were removed, surface water was gently blotted using absorbent tissue, and both weight and thickness were immediately remeasured.

Table 2. Compositions of Wood-plastic Composites in Experiment

Sample Code	HDPE (wt%)	Rubberwood Flour (wt%)	Coconut Shell Flour (wt%)	Palm Kernel Shell Flour (wt%)
H70R30	70	30	-	-
H60R40	60	40	-	-
H50R50	50	50	-	-
H70C30	70	-	30	-
H60C40	60	-	40	-
H50C50	50	-	50	-
H70P30	70	-	-	30
H60P40	60	-	-	40
H50P50	50	-	-	50

Mechanical and Physical Characterizations

Morphological analysis

A Scanning electron microscope (FEI Quanta 400, FEI Company, Hillsboro, OR, USA) was employed to examine the microstructures of rubberwood, coconut shell, and palm kernel shell, as well as to evaluate voids, interfacial adhesion, and dispersion of reinforcement materials within the plastic matrix. Before imaging, the cross-sectional surfaces of the samples were gold-coated using a sputter coater (SPI Module; Structure Probe, Inc., West Chester, PA, USA) to prevent electron charging. The SEM observations were conducted at an accelerating voltage of 20 kV with a magnification of 1000 \times .

Statistical analysis

The effect of filler content on the mechanical and physical properties of the composites was statistically analyzed using one-way analysis of variance (ANOVA), after which a comparison of the mean values was performed through Tukey's multiple comparison test to identify specific differences among groups. In addition, Student's *t*-tests were employed to examine significant variations between before and after immersion conditions of the WPC samples after eight weeks. All statistical evaluations were conducted at a 5% significance level ($\alpha = 0.05$).

Flexural test

The flexural behavior of the WPC specimens, including MOR and MOE, was evaluated in accordance with ASTM D 790-17 (2017), using a Mechanical Universal Testing Machine (Model NRI-TS500-50, Narin Instrument Co., Ltd., Samut Prakan, Thailand). Tests were conducted at a crosshead speed of 2 mm/min over an 80 mm support span. Rectangular specimens (13 mm \times 100 mm \times 4.8 mm) were prepared and tested at ambient room temperature of 25 °C with five replicates in each formulation and condition.

Screw withdrawal test

The screw withdrawal strength (SWS) of the WPC samples was measured in accordance with ASTM D 1037-12 (2020), using the same Universal Testing Machine as for the flexural test. The screw withdrawal test was conducted at a crosshead speed of 1.5 mm/min. The WPC specimens, with dimensions of 50 mm (width) \times 50 mm (length) \times 4.8 mm (thickness), were prepared with wood screws (diameter: 4.18 mm, threaded length: 50 mm) driven through their faces. The screws were embedded prior to immersing the specimens in water. The specimens were tested at ambient room temperature of 25 °C with five replicates in each formulation and condition.

Hardness test

The hardness of the WPC specimens was evaluated in accordance with ASTM D 2240-15 (2021), using a Shore D durometer (Model GS-702G, Teclock Corporation, Nagano, Japan). Specimens were prepared with nominal dimensions of 30 mm (width) \times 30 mm (length) \times 4.8 mm (thickness) and tested at ambient room temperature of 25 °C. For each formulation and condition, five replicate measurements were conducted. During testing, each specimen was positioned on a rigid, horizontal surface, and the durometer was applied vertically to ensure accurate readings.

Surface roughness measurement

The surface quality of the WPCs following immersing in water was assessed by measuring surface roughness using a Portable Surface Roughness Tester (Model SJ-210, Mitutoyo (Thailand) Co., Ltd., Bangkok, Thailand). Prior to measurement, the instrument was calibrated to ensure accuracy. The roughness parameter, specifically R_a , was used to evaluate the surface characteristics of the WPC samples. R_a represents the arithmetic mean of the absolute values of the profile heights along the evaluation length. Surface roughness values were obtained digitally, and measurements were conducted on five replicated WPC specimens at room temperature (25 °C).

Measurements of flexure, screw withdrawal, hardness, and surface roughness were repeated every 2 weeks throughout the water immersion period. The changes in mechanical and physical properties were monitored over an 8-week duration, in which the specimens reached saturation and ceased to absorb additional moisture.

RESULTS AND DISCUSSION

Morphology of the Natural Filler and Composites

The morphological characteristics of natural fillers, specifically rubberwood, coconut shell, and palm kernel shell, were examined using SEM imaging, as illustrated in Fig. 3. Rubberwood exhibited a fibrous and flaky structure with porous surfaces and fractured cell walls, indicating high surface roughness that may enhance mechanical interlocking with a plastic matrix (Schuberth *et al.* 2016; Islam and Hasan 2025). In contrast, coconut shell exhibited a denser morphology comprising angular particles and relatively smoother surfaces, which, while potentially reducing the specific surface area, can contribute to improved structural rigidity in the composites (Qian *et al.* 2013). Additionally, the palm kernel shell displayed a blocky and brittle morphology characterized by jagged edges and rough surfaces with visible microcracks. These surface features may facilitate mechanical adhesion, and the irregular structure further reflects the inherently brittle nature of this lignocellulosic filler.

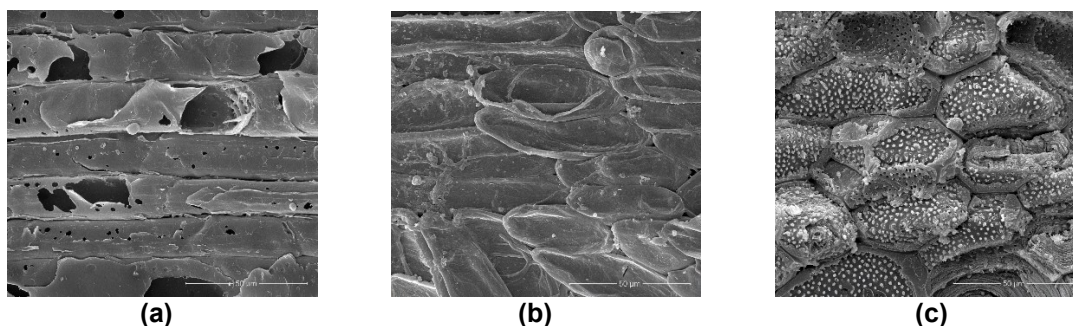


Fig. 3. SEM images (magnification 1000×) of the natural fillers: (a) rubberwood, (b) coconut shell, and (c) palm kernel shell

The SEM analyses of HDPE-based composites incorporating RWF, CSF, and PKSF, as depicted in Fig. 4, reveal distinct differences in filler dispersion and interfacial characteristics. In the case of RWF-filled composites (Fig. 4a), the fillers appeared relatively well-dispersed; however, small interfacial voids and micro-debonding regions were evident, reflecting the typical incompatibility between hydrophilic fillers and the

hydrophobic HDPE matrix. However, the fibrous structure of rubberwood likely facilitates mechanical interlocking. The CSF-filled composites (Fig. 4b) exhibited more uniform dispersion and fewer interfacial voids, which may be attributed to the angular morphology of the particles promoting physical anchorage within the matrix. Further, the PKSF composites (Fig. 4c) demonstrated the weakest interfacial bonding, with evident filler pull-outs and large interfacial gaps. These deficiencies are likely due to the brittle nature and smoother surfaces of the filler, which resist effective stress transfer (Gamstedt *et al.* 2011). Collectively, these findings underscore the critical role of filler morphology in influencing interfacial adhesion and the overall mechanical performance of WPCs. Fillers with rough or angular surfaces tend to enhance mechanical interlocking, whereas smooth or brittle particles are associated with poor matrix compatibility. This is consistent with previous studies reporting that both surface texture and dispersion quality are key determinants of mechanical performance in the WPCs (Salasińska and Ryszkowska 2015).

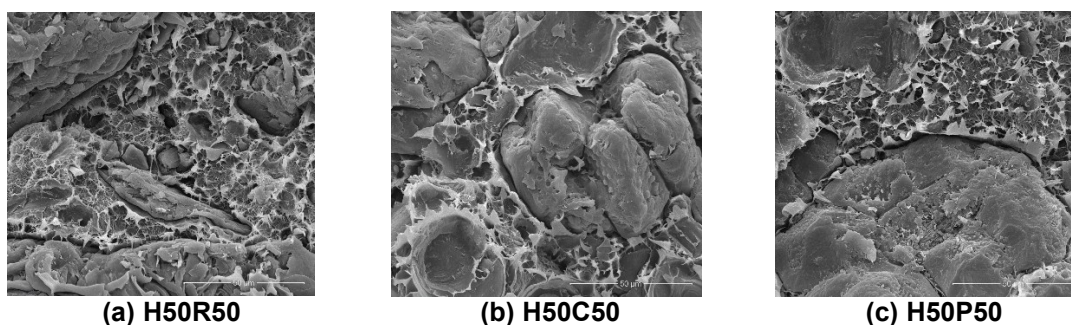


Fig. 4. SEM images (magnification 1000×) of HDPE composites reinforced with (a) rubberwood flour, (b) coconut shell flour, and (c) palm kernel shell flour

Mechanical Properties of the Composites

Figure 5 presents the effect of filler type and content (ranging from 30 to 50 wt%) on the MOR and MOE of HDPE-based composites reinforced with RWF, CSF, and PKSF. For all filler types, MOR exhibited a decreasing linear trend with increasing filler content for all filler types. This phenomenon is attributed to the weaker interfacial bonding between filler and plastic matrix with higher filler content, resulting from the nature incompatibility between the hydrophilic nature of filler and the hydrophobic character of the plastic matrix (Srivabut *et al.* 2024). Among the three, composites reinforced with RWF consistently displayed the highest MOR values across all filler concentrations, followed by those containing PKSF and CSF. This trend is quantitatively supported by linear regression models, with RWF-reinforced composites demonstrating the steepest decline ($y_R = -0.3769x + 35.52$, $R^2 = 0.9836$, and $p\text{-value} = 0.082$), indicating a higher sensitivity of MOR to filler loading. Composites with palm kernel shell ($y_P = -0.2578x + 28.815$, $R^2 = 0.9719$, and $p\text{-value} = 0.107$) and coconut shell ($y_C = -0.2143x + 25.512$, $R^2 = 0.9788$, and $p\text{-value} = 0.093$) displayed more gradual decreases. This was likely due to their initially lower MOR values, which are associated with differences in particle morphology and interfacial bonding efficiency.

In contrast, MOE increased linearly with higher filler content, reflecting improved stiffness attributed to rigid filler particles within the HDPE matrix (Bal 2022). The RWF-based composites exhibited the greatest improvement in stiffness, reaching approximately 2.06 GPa at 50 wt%, with strong correlation ($y_R = 0.0295x + 0.5721$, $R^2 = 0.9884$, and $p\text{-value} = 0.069$). The CSF-filled composites displayed intermediate stiffness gains ($y_C = 0.0183x + 0.8465$, $R^2 = 0.9963$, and $p\text{-value} = 0.039$), while PKSF-filled composites exhibited the lowest stiffness

improvement ($y_P = 0.0171x + 0.6416$, $R^2 = 0.9359$, and $p\text{-value} = 0.163$). The observed increases in MOE are primarily attributed to the rigidity of the lignocellulosic fillers and the improved load transfer from the HDPE matrix to the filler.

These results are consistent with a previous report that emphasizes the critical role of filler morphology, interfacial adhesion, and dispersion in determining the mechanical behavior of natural fiber-reinforced composites (Olonisakin *et al.* 2022). Specifically, fillers with rough or fibrous surfaces, such as RWF, promote superior mechanical interlocking and stress transfer, thereby enhancing mechanical strength. In contrast, smoother or more brittle particles, such as those from CSF and PKSf, tend to form weaker interfacial bonds, leading to comparatively inferior mechanical performance (Olonisakin *et al.* 2022).

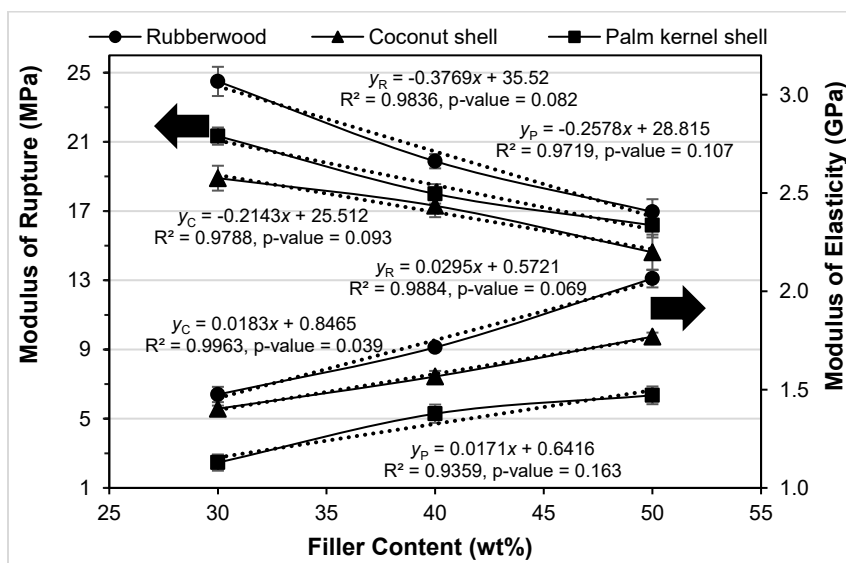


Fig. 5. Effect of filler types and contents on MOR and MOE of WPCs

Long-term Water Absorption and Thickness Swelling Behavior

Figures 6 and 7 demonstrate distinct effects of filler types and contents (30, 40, and 50 wt%) on long-term WA and TS behaviors of HDPE-based WPCs over an 8-week immersion period. In general, WA and TS values for all composites increased progressively with immersion time (Bera *et al.* 2019), eventually reaching equilibrium after approximately 4 weeks. The composites reinforced with RWF exhibited the highest water uptake, reaching approximately 12.5% at 50 wt% filler loading (H50R50). In comparison, the composites containing CSF showed the lowest WA, with values around 9.7% at the same filler content (H50C50). The PKSf-filled composites demonstrated intermediate absorption levels, measuring approximately 10.4% at H50P50. Similar trends were observed for TS, with RWF composites experiencing the greatest dimensional expansion (~10.3% at H50R50), confirming their lower dimensional stability upon moisture exposure. Likewise, the CSF composites exhibited the least swelling (~8.2% at H50C50), suggesting enhanced dimensional stability, which was likely due to their higher lignin content and lower porosity (Leng *et al.* 2024). The PKSf composites displayed intermediate swelling (~8.7% at H50P50) behavior, falling between the other two filler types. These differences can be explained by considering the chemical composition and density of the fillers (see Table 1). Rubberwood, characterized by relatively high cellulose (39%) and hemicellulose (29%) contents, contains more hydroxyl groups, which facilitate

water absorption and swelling through hydrogen bonding (Khamtree *et al.* 2023; Ayrilmis *et al.* 2025). Its lower density (480 to 650 kg/m³) may also contribute to increased porosity, further enhancing moisture uptake. Furthermore, coconut shell, with its notably intermediate lignin content (46%) and considerably higher density (1,310 kg/m³), exhibits greater hydrophobicity and structural compactness, limiting moisture penetration and consequently reducing WA and TS. Palm kernel shell, possessing the highest lignin content (50.5%) and high density (1,254 kg/m³), exhibited moisture absorption in comparison to those of rubberwood and coconut shell. Although palm kernel shell possesses the highest lignin content, its moisture absorption was greater than that of coconut shell. This suggests that hydrophobicity is not solely governed by lignin content but also influenced by filler morphology and microstructural compactness.

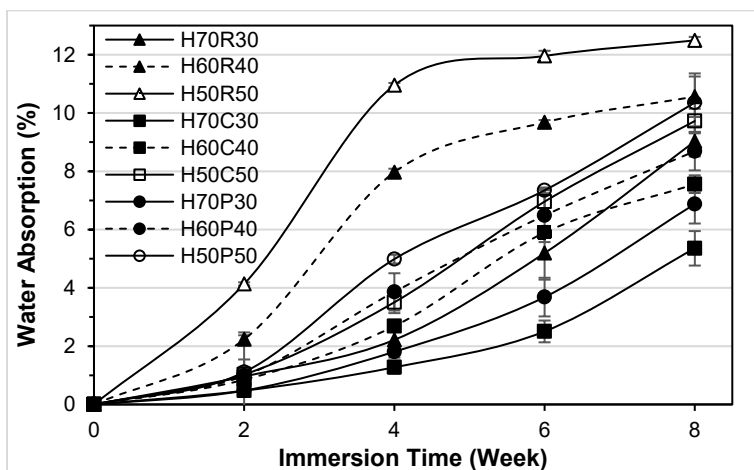


Fig. 6. Long-term water absorption behavior of WPCs

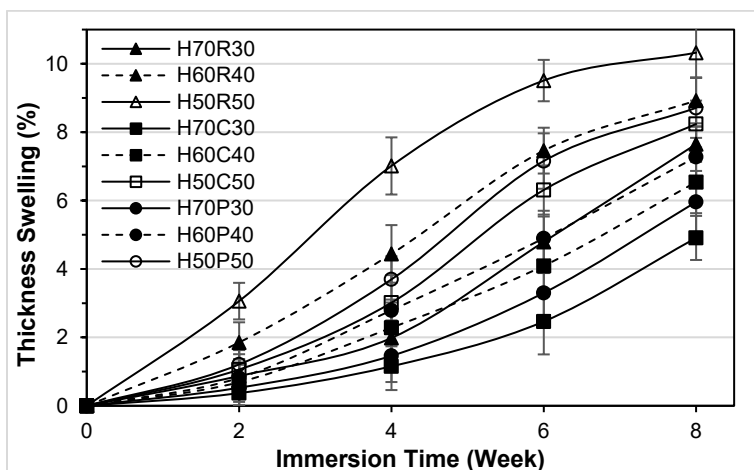


Fig. 7. Thickness swelling as a function of water immersion time for WPCs

Increasing filler content from 30 wt% to 50 wt% consistently enhanced WA and TS, regardless of filler type. This increase can be attributed to the greater number of hydrophilic sites from the lignocellulosic fillers (Bera *et al.* 2019), promoting more water uptake and subsequent dimensional changes. Higher filler loadings typically increase filler-to-filler contact and generate more interfacial voids and micro-pores, facilitating moisture penetration and swelling phenomena (Ayrilmis *et al.* 2025). Overall, the results clearly

demonstrate the importance of both filler type and content in controlling moisture-related performance of WPCs. Specifically, fillers with higher cellulose and hemicellulose contents and lower density, such as RWF, considerably increase moisture uptake and dimensional instability as filler content increases. Conversely, fillers rich in lignin and density, like CSF, effectively mitigate these effects, suggesting their potential advantage in moisture-sensitive composite applications. Therefore, strategic selection of filler type and optimization of filler loading levels are crucial for tailoring WPCs to achieve desired physical performance in practical applications.

Deterioration Behavior in the Mechanical and Physical Properties under Water Immersion

Flexural properties

Figures 8 and 9 illustrate the degradation behavior of flexural properties, namely MOR and MOE of HDPE-based WPCs reinforced with RWF, CSF, and PKSF, respectively, following water immersion for up to 8 weeks.

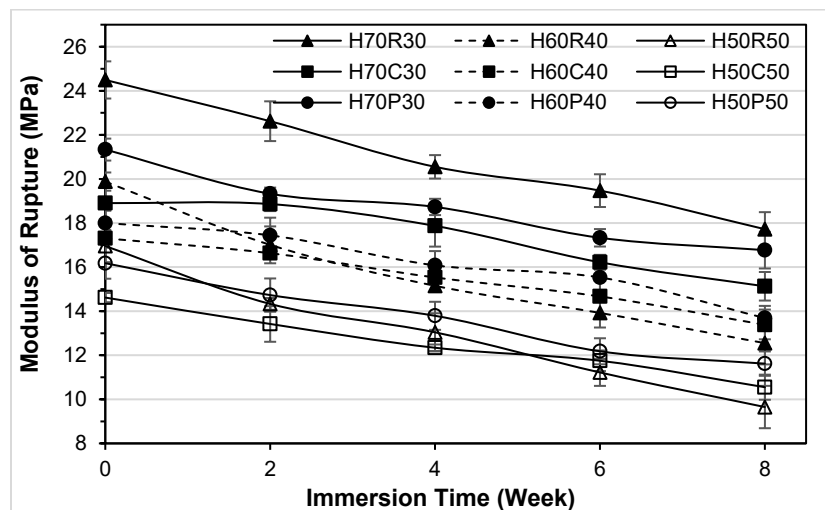


Fig. 8. Deterioration in MOR as a function of water immersion time for WPCs

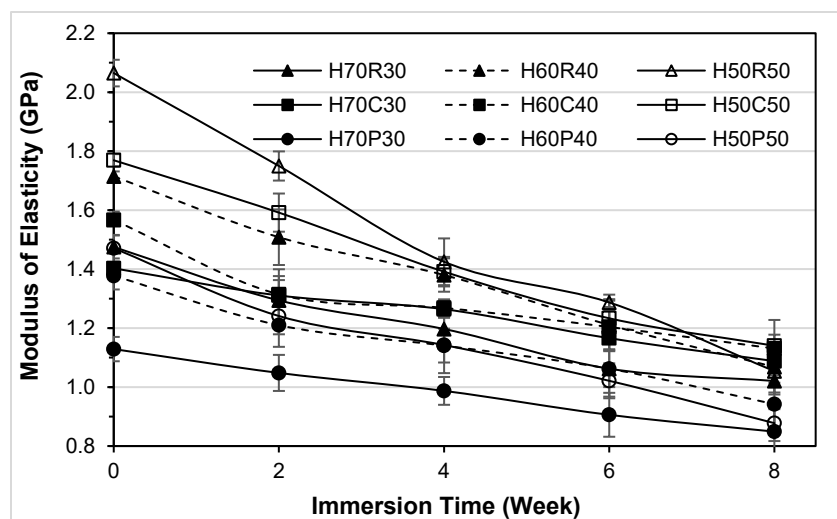


Fig. 9. Deterioration in MOE as a function of water immersion time for WPCs

A progressive reduction in both MOR and MOE was observed for all composite formulations, indicating water-induced weakening of the plastic-filler interface and a reduction in the composite's ability to bear and resist bending loads (Wang *et al.* 2020). At the initial (un-immersed) condition, the composites with higher filler contents, particularly at 50 wt% filler, exhibited enhanced MOE values, which can be attributed to the increased stiffness given by the rigid lignocellulosic fillers (Bal 2022). However, MOR tended to decline with increasing filler content, likely due to inefficient stress transfer at high filler loadings caused by inadequate matrix wetting and interfacial bonding (Bal 2023).

After immersion for 8 weeks, the deterioration of both MOR and MOE was markedly more severe in the composites with higher filler loadings. For instance, in RWF-filled composites, MOR loss increased from 38.2% (H70R30) to 75.7% (H50R50), while MOE loss increased dramatically from 44.5% to 95.9%, as indicated in Table 3. This considerable reduction is attributed to the hydrophilic nature of rubberwood, which contains high contents of cellulose and hemicellulose that facilitate water absorption, swelling, and interfacial debonding (Wang *et al.* 2020).

Table 3. Effect of Filler Contents and Water Immersion Times on Mechanical and Physical Properties of the WPCs

Sample code	MOR (MPa)			MOE (GPa)			SWS (MPa)		
	0 W	8 W	%loss	0 W	8 W	%loss	0 W	8 W	%loss
H70R30	24.5 ^{Aa}	17.7 ^{Ba}	38.2	1.48 ^{Aa}	1.02 ^{Ba}	44.5	22.8 ^{Aa}	15.9 ^{Ba}	43.5
H60R40	19.9 ^{Ab}	12.5 ^{Bb}	58.4	1.71 ^{Ab}	1.07 ^{Ba}	60.5	19.6 ^{Ab}	11.5 ^{Bb}	70.9
H50R50	17.0 ^{Ac}	9.65 ^{Bc}	75.7	2.06 ^{Ac}	1.05 ^{Ba}	95.9	17.3 ^{Ac}	7.85 ^{Bc}	120
<i>p-value</i>	<i>0.001*</i>	<i>0.000*</i>	-	<i>0.000*</i>	<i>0.142</i>	-	<i>0.000*</i>	<i>0.000*</i>	-
H70C30	18.9 ^{Aa}	15.1 ^{Ba}	24.9	1.40 ^{Aa}	1.09 ^{Ba}	28.9	18.0 ^{Aa}	14.5 ^{Ba}	24.4
H60C40	17.3 ^{Aa}	13.4 ^{Ba}	29.3	1.57 ^{Ab}	1.13 ^{Bb}	38.5	17.2 ^{Aa}	12.4 ^{Bb}	38.8
H50C50	14.6 ^{Ab}	10.5 ^{Bb}	38.5	1.77 ^{Ac}	1.14 ^{Bb}	55.2	15.5 ^{Ab}	10.5 ^{Bc}	47.6
<i>p-value</i>	<i>0.024*</i>	<i>0.017*</i>	-	<i>0.001*</i>	<i>0.041*</i>	-	<i>0.002*</i>	<i>0.000*</i>	-
H70P30	21.3 ^{Aa}	16.8 ^{Ba}	27.2	1.13 ^{Aa}	0.85 ^{Ba}	32.9	20.1 ^{Aa}	15.5 ^{Ba}	30.2
H60P40	18.0 ^{Ab}	13.7 ^{Bb}	31.4	1.38 ^{Ab}	0.94 ^{Bb}	46.2	18.5 ^{Aa}	13.0 ^{Bb}	42.1
H50P50	16.2 ^{Ac}	11.6 ^{Bc}	39.2	1.47 ^{Ac}	0.88 ^{Ba}	67.6	16.2 ^{Ab}	10.2 ^{Bc}	58.3
<i>p-value</i>	<i>0.001*</i>	<i>0.002*</i>	-	<i>0.000*</i>	<i>0.037*</i>	-	<i>0.000*</i>	<i>0.000*</i>	-

Sample code	Hardness (Shore D)			Surface roughness (μm)		
	0 W	8 W	%loss	0 W	8 W	%loss
H70R30	53.2 ^{Aa}	43.2 ^{Ba}	23.2	1.87 ^{Aa}	2.53 ^{Ba}	35.3
H60R40	55.2 ^{Ab}	43.8 ^{Ba}	26.0	1.92 ^{Aab}	2.68 ^{Bb}	40.1
H50R50	59.0 ^{Ac}	44.6 ^{Ba}	32.3	1.95 ^{Ab}	2.80 ^{Bc}	44.0
<i>p-value</i>	<i>0.015*</i>	<i>0.258</i>		<i>0.017*</i>	<i>0.000*</i>	
H70C30	52.0 ^{Aa}	43.6 ^{Ba}	19.4	1.71 ^{Aa}	2.23 ^{Ba}	30.6
H60C40	54.1 ^{Ab}	44.4 ^{Ba}	21.9	1.80 ^{Aab}	2.39 ^{Ba}	32.5
H50C50	58.4 ^{Ac}	46.2 ^{Bb}	26.4	1.88 ^{Ab}	2.59 ^{Bb}	37.7
<i>p-value</i>	<i>0.004*</i>	<i>0.032*</i>		<i>0.006*</i>	<i>0.000*</i>	
H70P30	50.6 ^{Aa}	42.0 ^{Ba}	20.4	1.61 ^{Aa}	2.07 ^{Ba}	28.9
H60P40	53.3 ^{Ab}	43.6 ^{Ba}	22.1	1.70 ^{Aab}	2.22 ^{Bb}	30.8
H50P50	58.0 ^{Ac}	45.0 ^{Bb}	28.9	1.86 ^{Ab}	2.47 ^{Bc}	32.8
<i>p-value</i>	<i>0.000*</i>	<i>0.028*</i>		<i>0.001*</i>	<i>0.000*</i>	

Note: W = Week; MOR = Modulus of rupture; MOE = Modulus of elasticity; SWS = Screw withdrawal strength; *Filler contents significantly affected the measured properties at p -value < 0.05. Means within each column followed by the same superscripts (a-c) were not significantly different according to Turkey's test at α = 0.05. Different superscripts (A-B) of each property and formulation indicate significant difference (α = 0.05) between mechanical properties of the WPCs immersed for 0 and 8 weeks; % loss was calculated based on values obtained after 8 weeks of immersion.

However, the composites reinforced with CSF demonstrated superior resistance to water-induced degradation. The MOR losses ranged from 24.9% (H70C30) to 38.5% (H50C50), while MOE losses increased modestly from 28.9% to 55.2% as filler content increased from 30 wt% to 50 wt%. The superior stability of these composites can be attributed largely to the high lignin content (46%) and high density of coconut shell, which limits water permeability and promotes stronger filler-matrix bonding. Further, the PKSF composites displayed an intermediate performance between the rubberwood and coconut shell systems. The reduction in MOR ranged from 27.2% (H70P30) to 39.2% (H50P50), and MOE losses ranged from 32.9% to 67.6%. These findings highlight a moderate sensitivity to moisture and emphasize the combined influence of filler morphology and chemical composition on the long-term mechanical performance of WPCs under wet conditions.

Furthermore, the results of the one-way ANOVA revealed that filler content displayed a statistically significant influence ($p < 0.05$) on the MOR and MOE of all WPC formulations, both prior to immersion (0 W) and after eight weeks of water exposure (8 W), as presented in Table 3. Tukey's multiple comparison test also indicated that composites reinforced with 30 wt% rubberwood flour (suffix a) exhibited a significantly greater MOR compared to those containing 40 wt% (suffix b) and 50 wt% (suffix c) filler. Additionally, the 40 wt% formulation (suffix b) demonstrated a markedly higher MOR than the 50 wt% formulation (suffix c). Student's t test in Table 3 further confirmed that the unimmersed specimens (suffix A) possessed significantly higher MOR and MOE values than the samples subjected to eight weeks of immersion (suffix B).

Screw withdrawal property

Figure 10 illustrates the deterioration in SWS of HDPE-based WPCs as a function of water immersion time for varying filler types and loadings. A general decreasing trend in SWS was observed for all formulations with increased immersion duration, reflecting the adverse effects of water uptake on the interfacial bonding and structural integrity of the composites (Homkhiew *et al.* 2016).

Among the different filler types, the composites containing CSF exhibited the highest resistance to moisture-induced deterioration. For instance, the H50C50 formulation maintained relatively high SWS values, decreasing from approximately 15.5 MPa before immersion to around 10.5 MPa by 8 weeks (SWS loss of 47.6%). This superior performance is attributed to the high lignin content (46%) and dense microstructure of coconut shell particles, which provide enhanced moisture resistance and interfacial stability. In contrast, RWF composites displayed the steepest deterioration in SWS with increasing immersion time. At 50 wt% RWF content, the H50R50 composites exhibited a reduction from 17.3 to 7.85 MPa over the 8-week period, corresponding to a 120% loss. This considerable reduction can be linked to the higher hydrophilicity of RWF, which contains more cellulose and hemicellulose (see in Table 1), leading to greater water uptake and weakened filler-matrix bonding (Wang *et al.* 2020).

The PKSF composites demonstrated intermediate behavior. The H50P50 composites showed a decline in SWS from 16.2 to 10.2 MPa, also a 58.3% loss. These observations highlight the critical role of filler selection in optimizing the long-term mechanical durability of WPCs exposed to wet environments.

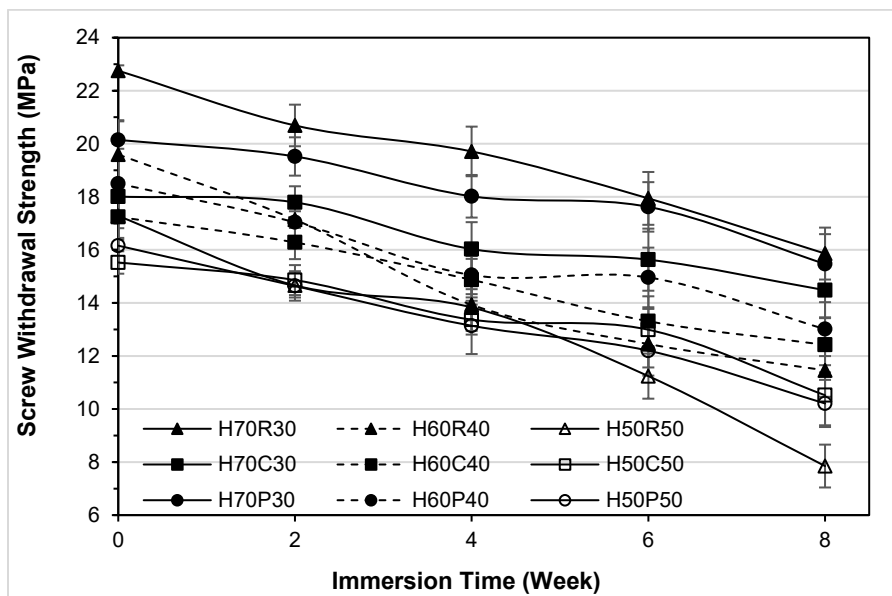


Fig. 10. Deterioration in SWS as a function of water immersion time for WPCs

The effect of filler content was also clearly evident. Prior to immersion, the composites containing 30 wt% filler consistently exhibited higher SWS than those with 40 and 50 wt% filler of the same type. This trend suggests that excessive filler loading may lead to agglomeration, poor dispersion, or increased interfacial defects (Ejeta 2023), all of which reduce the material's ability to securely hold fasteners. Further, the results clearly demonstrate that increasing the filler content from 30 wt% to 50 wt% led to considerably greater deterioration in SWS, regardless of filler type. Among the RWF composites, the SWS loss increased markedly from 43.5% (H70R30) to 120% (H50R50). A similar progressive degradation pattern was observed in the PKSf and CSf composites, with losses rising from 30.2% to 58.3% and 24.4% to 47.6%, respectively. The higher extent of SWS degradation at elevated filler loadings (50 wt%) is likely due to the increased number of hydrophilic sites, larger interfacial areas, and more extensive filler-filler contact regions (Shahapurkar *et al.* 2024). These conditions create microstructural pathways that facilitate water penetration, thereby accelerating interfacial debonding and matrix deterioration during immersion. Additionally, excessive filler can lead to poor dispersion and inadequate wetting by the polymer matrix (Olonisakin *et al.* 2022), further compromising the composite's resistance to moisture-induced damage. This trend highlights the adverse effect of excessive filler loading on the long-term durability of WPCs in moist environments. Optimizing both filler type and content is thus essential for moisture-resistant applications for which fastener retention is critical.

Hardness property

Figure 11 shows the variation in Shore D hardness of HDPE-based WPCs reinforced with RWF, CSf, and PKSf at filler contents of 30, 40, and 50 wt%, over water immersion periods of 8 weeks. In all cases, hardness decreased with increasing immersion time, indicating the softening and deterioration of the plastic-filler interfacial region due to water uptake (Mysiukiewicz and Sterzyński 2017). Prior to immersion, the composites with higher filler contents, particularly those with 50 wt%, exhibited the highest initial hardness values. This is expected due to the inherent stiffening effect of the fillers (Homkhiew *et al.*

2024). For example, the H50P50 composites showed approximately 14.6% higher hardness compared to its 30 wt% (H70P30), indicating the effectiveness of increased filler content in reinforcing the composite under dry conditions. However, this trend reversed upon long-term immersion. After 8 weeks of water immersion, the composites with higher filler loadings experienced considerably greater percentage losses in hardness compared to those with lower filler contents. The hardness loss of RWF composites increased dramatically from 23.2% at 30 wt% RWF (H70R30) to 32.3% at 50 wt% RWF (H50R50). Similarly, CSF-filled WPCs showed an increase in %loss from 19.4% (H70C30) to 26.4% (H50C50), while %loss of PKSf composites increased from 20.4% to 28.9% over the same range. This behavior can be attributed to the plasticization of the natural filler upon moisture absorption, which increases its softness and consequently reduces the hardness of the composites (Homkhiew *et al.* 2016).

This degradation behavior is attributed to the combined effects of increased hydrophilic sites, greater filler-matrix interfacial area, and potentially poorer dispersion at higher filler loadings (Homkhiew *et al.* 2016). As filler content increases, the number of microvoids and interfacial regions rises, which act as pathways for water access. For hydrophilic fillers such as the rubberwood (rich in cellulose and hemicellulose, see in Table 1), the absorbed moisture weakens interfacial adhesion and reduces surface hardness (Khamtree *et al.* 2023). In contrast, the coconut shell, with its high lignin content (46%) and dense morphology, showed the lowest hardness loss, indicating better resistance to water-induced softening.

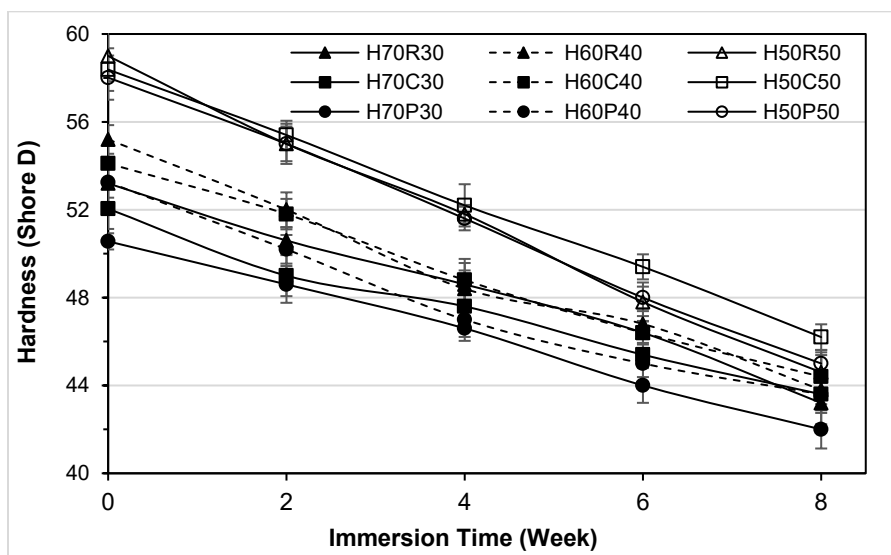


Fig. 11. Deterioration in hardness as a function of water immersion time for WPCs

Surface roughness property

Figure 12 illustrates the change in surface roughness of WPCs as a function of water immersion time (0 to 8 weeks) and different natural filler types and contents. A consistent increase in surface roughness was observed for all composite formulations, with the degree of increase varying depending on both the filler type and loading. Under prior to immersion conditions, the composites with higher filler content (50 wt%) exhibited slightly higher roughness due to the increased exposure of filler particles, larger interior void space, and greater surface heterogeneity (Ayrilmis *et al.* 2012). After 8 weeks of immersion, all composites exhibited a marked increase in surface roughness, which is likely a

consequence of sequential degradation mechanisms involving moisture-induced swelling, followed by plastic matrix softening and subsequent interfacial debonding between the filler and matrix (Tasdemir *et al.* 2020). Further, the surface roughness consistently rose with higher filler content for all filler types. For instance, in RWF-filled composites, the surface roughness increased from 35.3% in H70R30 to 44.0% in H50R50. A similar behavior was observed in the CSF composites where surface roughness increased from 30.6% to 37.7%, and in the PKSf composites that rose from 28.9% to 32.8% as the filler content increased from 30 wt% to 50 wt%. This trend indicates that higher filler loadings expanded the exposed surface area and filler-matrix interfacial regions, which were more vulnerable to water-induced degradation such as surface fibrillation, microcracking, and localized erosion (Sookyung *et al.* 2025).

Among the different filler types, the RWF composites showed the highest increase in surface roughness, which is consistent with its higher cellulose and hemicellulose content, components known to absorb water readily and contribute to surface swelling and degradation (Islam and Hasan 2025). By contrast, the PKSf and CSF composites exhibited lower increases in surface roughness. This was likely due to their higher lignin content and denser structure, which provides greater resistance to moisture-induced surface damage. Moreover, the optical microscopy images presented in Table 4 further support the surface roughness findings. Prior to immersion, all composite surfaces exhibited slight roughness. After 4 weeks of water immersion, increasing roughness was visible, particularly in samples with higher filler content. By 8 weeks, severe surface degradation was observed, especially in the composites with 50 wt% filler, which showed microvoids, crack propagation, and filler pull-out zones. This indicates interfacial debonding and material washout due to water penetration (Ratanawilai and Srivabut 2022). Further, the composites reinforced with CSF, such as H50C50, exhibited comparatively smoother surface changes even after immersion. Likewise, the PKSf-filled composites demonstrated moderate surface alterations, including localized roughening; however, these changes were less severe than those observed in the RWF composites.

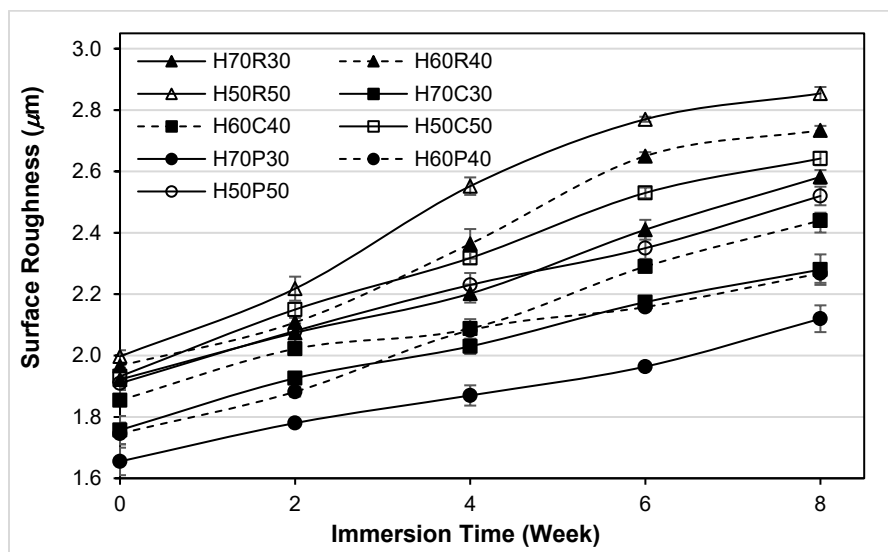
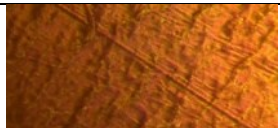
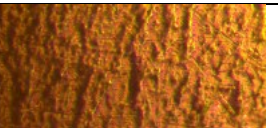
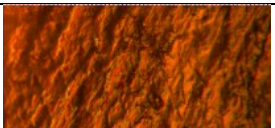
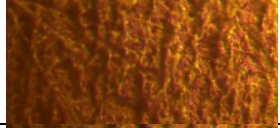
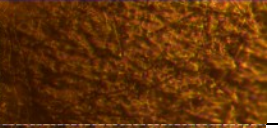
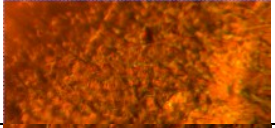
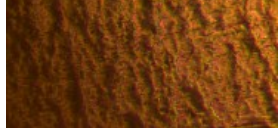
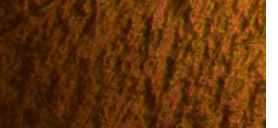
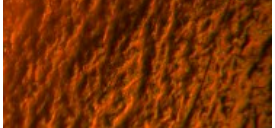
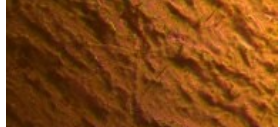
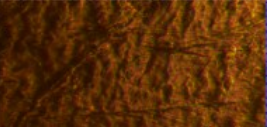
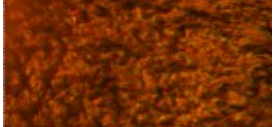
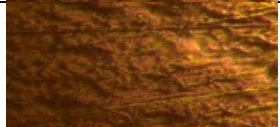
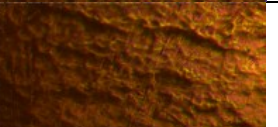
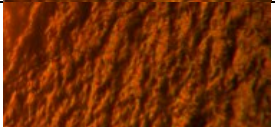

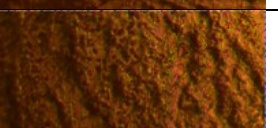
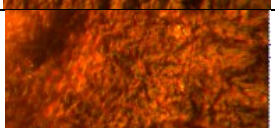


Fig. 12. Deterioration in surface roughness as a function of water immersion time for WPCs

Table 4. Optical Microscopy Images of the Composite Surfaces at Different Immersion Stages

Condition	Prior to immersion	Immersed for 4 weeks	Immersed for 8 weeks
H70R30			
H50R50			
H70C30			
H50C50			
H70P30			
H50P50			

CONCLUSIONS

1. This work systematically evaluated the effects of filler type and content on the physical, mechanical, and moisture-resistance performance of high density polyethylene (HDPE)-based wood-plastic composites (WPCs) reinforced with rubberwood flour (RWF), coconut shell flour (CSF), and palm kernel shell flour (PKSF). The results revealed that filler morphology, density, and chemical composition influenced interfacial adhesion and the composites' resistance to water-induced deterioration.
2. Among the reinforcements evaluated, CSF showed superior performance in mitigating moisture-related degradation. The CSF-filled composites exhibited the lowest water absorption, thickness swelling, and deterioration in modulus of rupture (MOR), modulus of elasticity (MOE), screw withdrawal strength (SWS), hardness, and surface roughness during prolonged water immersion. This behavior was attributed to CSF's high lignin content and dense, angular morphology, which enhanced filler-matrix bonding and limited moisture permeability.
3. Although RWF-reinforced composites initially exhibited considerable mechanical strength, they demonstrated pronounced delicacy to moisture-induced degradation, particularly at elevated filler loadings. The PKSF composites showed intermediate

behavior, reflecting a balance between stiffness enhancement and moderate water resistance.

4. Overall, this work highlights the potential of using high-density lignocellulosic fillers, such as CSF and PKSf, to develop durable, water-resistant WPCs, while simultaneously valorizing agricultural by-products within a circular material economy.
5. The concept of incorporating hybrid filler systems, such as a combination of CSF and RWF, offers an interesting pathway to balance cost and performance in WPCs. The inclusion of fine CSF particles could improve interfacial adhesion and dimensional stability, while the coarser RWF could contribute to stiffness and load-bearing capacity. Moreover, the use of mixed fillers may reduce the overall filler cost due to the partial replacement of high-cost or limited-availability materials. Although this approach was not examined in the present study, it represents a promising direction for future research aimed at optimizing mechanical and physical properties through filler synergy.
6. From a practical perspective, the use of CSF and PKSf as alternative fillers can improve stiffness and reduce water absorption. However, their large-scale application may be constrained by higher processing energy demands. Thus, while these fillers show potential for enhanced composite performance, their cost-effectiveness and processing feasibility require further evaluation for industrial implementation.

ACKNOWLEDGMENTS

The authors would like to sincerely thank the Faculty of Engineering, Rajamangala University of Technology Srivijaya, for providing research facilities. We would also like to thank Mr. Saharat Leamkeaw and Mr. Kankawee Choosuwan for supporting this work. In addition, we would like to declare that generative AI (ChatGPT-4.0) was used solely for assistance in checking and refining the English language in this manuscript.

REFERENCES CITED

- Anuchi, S. O., Campbell, K. L. S., and Hallett, J. P. (2022). "Effective pretreatment of lignin-rich coconut wastes using a low-cost ionic liquid," *Sci. Rep.* 12, article 6108. <https://doi.org/10.1038/s41598-022-10017-3>
- ASTM D 570-98 (1998). "Standard test method for water absorption of plastics," ASTM International, West Conshohocken, PA, USA.
- ASTM D 790-17 (2017). "Standard test methods for flexural properties of unreinforced and reinforced plastics and electrical insulating materials," ASTM International, West Conshohocken, PA, USA.
- ASTM D 1037-12 (2020). "Standard test methods for evaluating properties of wood-base fiber and particle panel materials," ASTM International, West Conshohocken, PA, USA.
- ASTM D 2240-15 (2021). "Standard test method for rubber property-durometer hardness," ASTM International, West Conshohocken, PA, USA.
- Ayrlmis, N., Benthien, J. T., and Thoemen, H. (2012). "Effects of formulation variables on surface properties of wood plastic composites," *Compos. Part B: Eng.* 43(1), 325-331. <https://doi.org/10.1016/j.compositesb.2011.07.011>

- Ayrilmis, N., Yurttas, E., Avsar, E. Y., Kahraman, M. V., Özdemir, F., Palanisamy, S., Yetiş, F., Ali, S. K., Gurusamy, M. K., Palaniappan, M., *et al.* (2025). “Properties of plastic composites filled with giant reed flour and magnesium oxide nanoparticles,” *BioResources* 20(2), 2670-2686. <https://doi.org/10.15376/biores.20.2.2670-2686>
- Bal, B. (2022). “Mechanical properties of wood-plastic composites produced with recycled polyethylene, used Tetra Pak® boxes, and wood flour,” *BioResources* 17(4), 6569-6577. <https://doi.org/10.15376/biores.17.4.6569-6577>
- Bal, B. (2023). “Some mechanical properties of WPCs with wood flour and walnut shell flour,” *Polimeros* 33(2), article e20230020. <https://doi.org/10.1590/0104-1428.20230005>
- Bera, T., Mohanta, N., Prakash, V., Pradhan, S., and Acharya, S. K. (2019). “Moisture absorption and thickness swelling behaviour of luffa fibre/epoxy composite,” *J. Reinfor. Plast. Compos.* 38(19-20), 923-937. <https://doi.org/10.1177/0731684419856703>
- Chen, L., Gao, F., Liu, J., Li, D., Chen, D., Li, Y., Hao, X., Ou, R., Wang, Q. (2025). “Enhancing wood-plastic composites for high-performance structural applications,” *Compos. Part B- Engineering* 299, article 112410. <https://doi.org/10.1016/j.compositesb.2025.112410>
- Dagwa, I. M., and Ibhado, A. O. (2008). “Some physical and mechanical properties of palm kernel shell (PKS),” *Botswana J. Technol.* 17(2), article 52206. <https://doi.org/10.4314/bjt.v17i2.52206>
- Daud, S., Ismail, H., and AbuBakar, A. (2016). “Soil burial study of palm kernel shell-filled natural rubber composites: The effect of filler loading and presence of silane coupling agent,” *BioResources* 11(4), 8686-8702. <https://doi.org/10.15376/biores.11.4.8686-8702>
- Ejeta, L. O. (2023). “Nanoclay/organic filler-reinforced polymeric hybrid composites as promising materials for building, automotive, and construction applications – A state-of-the-art review,” *Compos. Interfaces.* 30(12), 1363-1386. <https://doi.org/10.1080/09276440.2023.2220217>
- Gamstedt, E. K., Sandell, R., Berthold, F., Pettersson, T., and Nordgren, N. (2011). “Characterization of interfacial stress transfer ability of particulate cellulose composite materials,” *Mech. Mater.* 43(11), 693-704. <https://doi.org/10.1016/j.mechmat.2011.06.015>
- Guo, J., Cao, M., Ren, W., Wang, H., Yu, Y. (2021). “Mechanical, dynamic mechanical and thermal properties of TiO₂ nanoparticles treatment bamboo fiber-reinforced polypropylene composites,” *J. Mater. Sci.* 56, 12643-12659. <https://doi.org/10.1007/s10853-021-06100-z>
- Homkhiew, C., Khamtree, S., Srivabut, C., and Petdee, T. (2024). “Biocomposite materials from natural rubber/polylactic acid blends reinforced rubberwood sawdust for producing children's toys,” *Clean. Eng. Technol.* 22, article 100803. <https://doi.org/10.1016/j.clet.2024.100803>
- Homkhiew, C., Ratanawilai, T., and Thongruang, W. (2016). “Long-term water absorption and dimensional stability of composites from recycled polypropylene and rubberwood flour,” *J. Thermoplast. Compos. Mater.* 29(1), 74-91. <https://doi.org/10.1177/0892705712475015>
- Islam, S., and Hasan, M. B. (2025). “An overview of the effects of water and moisture absorption on the performance of hemp fiber and its composites,” *Plants, People, Planet* 6(1), article e10167. <https://doi.org/10.1002/pls2.10167>

- Khamtree, S., Srivabut, C., Homkhiew, C., Ratanawilai, T., and Rawangwong, S. (2023). "The mechanical properties deterioration of rubberwood-latex sludge flour reinforced polypropylene composites after immersing in different water conditions," *Eur. J. Wood Wood Prod.* 81, 1223-1237. <https://doi.org/10.1007/s00107-023-01950-7>
- Lim, S. C., Gan, K. S., and Choo, K. T. (2003). "The characteristics, properties and uses of plantation timbers – Rubberwood and *Acacia mangium*," Timber Technology Bulletin No. 26, Timber Technology Centre, Forest Research Institute Malaysia, Kuala Lumpur, Malaysia.
- Mysiukiewicz, O., and Sterzyński, T. (2017). "Influence of water on tribological properties of wood-polymer composites," *Arch. Mech. Tech. Mater.* 37, 79-84.
- Olonisakin, K., Fan, M., Xin-Xiang, Z., Ran, L., Lin, W., Zhang, W., and Wenbin, Y. (2022). "Key improvements in interfacial adhesion and dispersion of fibers/fillers in polymer matrix composites; Focus on PLA matrix composites," *Compos. Interfaces* 29(10), 1071-1120. <https://doi.org/10.1080/09276440.2021.1878441>
- Petchpradab, P., Yoshida, T., Charinpanitkul, T., and Matsumura, Y. (2009). "Hydrothermal pretreatment of rubber wood for the saccharification process," *Ind. Eng. Chem. Res.* 48(9), 4587-4591. <https://doi.org/10.1021/ie801973x>
- Qian, H., Kucernak, A. R., Greenhalgh, E. S., Bismarck, A., and Shaffer, M. S. P. (2013). "Multifunctional structural supercapacitor composites based on carbon aerogel modified high performance carbon fiber fabric," *ACS Appl. Mater. Interfaces* 5(13), 6113-6122. <https://doi.org/10.1021/am400947j>
- Ratanawilai, T., and Srivabut, C. (2022). "Physico-mechanical properties and long-term creep behavior of wood-plastic composites for construction materials: Effect of water immersion times," *Case Stud. Constr. Mater.* 16, article e00791. <https://doi.org/10.1016/j.cscm.2021.e00791>
- Salasinska, K., and Ryszkowska, J. (2015). "The effect of filler chemical constitution and morphological properties on the mechanical properties of natural fiber composites," *Compos. Interfaces* 22(1), 39-50. <https://doi.org/10.1080/15685543.2015.984521>
- Schuberth, A., Göring, M., Lindner, T., Töberling, G., Puschmann, M., Riedel, F., Scharf, I., Schreiter, K., Spange, S., and Lampke, T. (2016). "Effect of new adhesion promoter and mechanical interlocking on bonding strength in metal-polymer composites," *IOP Conf. Ser.- Mater. Sci. Eng.* 118, article 012041. <https://doi.org/10.1088/1757-899X/118/1/012041>
- Sekhon, S. S., Kaur, P., and Park, J.-S. (2021). "From coconut shell biomass to oxygen reduction reaction catalyst: Tuning porosity and nitrogen doping," *Renew. Sustain. Energy Rev.* 147, article ID 111173. <https://doi.org/10.1016/j.rser.2021.111173>
- Shahapurkar, K., Gebremaryam, G., Kanaginahal, G., Ramesh, S., Nik-Ghazali, N. N., Chenrayan, V., Soudagar, M. E. M., Fouad, Y., and Kalam, M. A. (2024). "An experimental study on the hardness, inter laminar shear strength, and water absorption behavior of Habeshian banana fiber reinforced composites," *J. Nat. Fibers* 21(1), article 2338930. <https://doi.org/10.1080/15440478.2024.2338930>
- Srivabut, C., Rawangwong, S., Hiziroglu, S., and Homkhiew, C. (2024). "Multi-objective optimization of turning process parameters and wood sawdust contents using response surface methodology for the minimized surface roughness of recycled plastic/wood sawdust composites," *Compos. Part C- Open Access* 14, article 100477. <https://doi.org/10.1016/j.jcomc.2024.100477>

- Tasdemir, C., Basboga, I. H., and Hiziroglu, S. (2020). "Surface quality of wood plastic composites as function of water exposure," *Appl. Sci.* 10, article 5122. <https://doi.org/10.3390/app10155122>
- Wang, W., Guo, X., Zhao, D., Liu, L., Zhang, R., and Yu, J. (2020). "Water absorption and hygrothermal aging behavior of wood-polypropylene composites," *Polymers* 12(4), article 782. <https://doi.org/10.3390/polym12040782>

Article submitted: September 2, 2025; Peer review completed: October 5, 2025; Revised version received: October 20, 2025; Accepted: December 5, 2025; Published: December 15, 2025.

DOI: 10.15376/biores.21.1.1030-1049